

Nonlocal Drag Thermoelectricity Generated by Ferroelectric Heterostructures

Ping Tang¹, Ken-ichi Uchida^{2,3}, and Gerrit E. W. Bauer^{1,3,4,5,6}

¹WPI-AIMR, Tohoku University, 2-1-1 Katahira, Sendai 980-8577, Japan

²National Institute for Materials Science, Tsukuba 305-0047, Japan

³Institute for Materials Research, Tohoku University, 2-1-1 Katahira, Sendai 980-8577, Japan

⁴Center for Spintronics Research Network, Tohoku University, Sendai 980-8577, Japan

⁵Zernike Institute for Advanced Materials, University of Groningen, 9747 AG Groningen, Netherlands and

⁶Kavli Institute for Theoretical Sciences, University of the Chinese Academy of Sciences, Beijing 10090, China

The “ferron” excitations of the electric-dipolar order carry energy as well as electric dipoles. Here we predict a nonlocal ferron drag effect in a ferroelectric on top of a metallic film: An electric current in the conductor generates a heat current in the ferroelectric by long-range charge-dipole interactions. The non-local Peltier and its reciprocal Seebeck effect can be controlled by electric gates and detected thermographically. We predict large effects for van der Waals ferroelectric films on graphene.

The electron-electron interaction between closely spaced two-dimensional electron gases (2DEGs) gives rise to *non-local* Coulomb drag effects [1–3], in which a current in an active layer induces a voltage over the passive one. The concept of Coulomb drag has been extended to other systems and interactions. A *local* drag effect by the electron-phonon interaction contributes to the thermopower in bulk conductors [4–7] and also a non-local drag effect can be mediated by phonons in the spacer between the 2DEGs [8–10]. In ferromagnetic metals, magnons, the quasiparticle excitations of local magnetization, transfer their momenta to conduction electrons by the exchange interaction. This local magnon drag effect enhances the Seebeck and Peltier coefficients [11–16]. The voltage in one layer induced by a current in the other in a heavy metal/ferromagnetic insulator/heavy metal stack is a non-local drag effect caused by spin Hall effect [17–19]. Theory predicts that magnons in magnetic films separated by a vacuum barrier experience a non-local drag effect by the magnetodipolar interaction [20]. The magnetodipolar interaction can also mediate an energy transfer through an air gap [21], but a non-local magnon drag effect has not yet been observed.

Ferroelectrics exhibit an electrically switchable spontaneous polarization that orders below a Curie temperature. Recently, we introduced “ferrons”, the bosonic excitations of ferroelectric order that carry elementary electric dipoles in the presence of transverse [22, 23] or longitudinal fluctuations [24]. A direct experimental observation of the predicted polarization and heat transport phenomena, e.g. by the transient Peltier effect [22] and associated stray fields [23], may not be so simple, however.

Here we pursue ideas to simplify the detection of ferronic effects via non-local thermoelectric drag effects in bilayers of a ferroelectric and a metal, which opens new strategies for heat-to-electricity conversion. We consider a film of a perpendicularly polarized ferroelectric insulator on top of an extended metallic sheet that experiences a “ferron drag” in the form of a non-local Peltier effect,

i.e., a heat current in the ferroelectric generated by an electric current in the metal film (see figure 1). We assume that the electric dipoles are all located in a common plane and that the electrons in the metal move in a parallel plane. This two-dimensional (2D) assumption is valid when the two films are separated by a distance d much larger than their thickness, but certainly appropriate when the conductor is, e.g., graphene and the ferroelectric a van der Waals mono- or bilayer [25–32].

The linear response relations of transport or Ohm’s Law in our bilayer (in the x -direction) connect four driving forces, i.e. an in-plane electric field E_M in the metal, a gradient of an out-of-plane electric field ∂E_{FE} in the ferroelectric, and independent temperature gradients in the two films, with the charge current j_c in the metal, polarization current j_p in the ferroelectric and the heat currents $j_q^{(M)}$ and $j_q^{(FE)}$:

$$\begin{pmatrix} -j_c \\ j_q^{(M)} \\ -j_p \\ j_q^{(FE)} \end{pmatrix} = \begin{pmatrix} L_{11} & L_{12} & L_{13} & L_{14} \\ L_{12} & L_{22} & L_{23} & L_{24} \\ L_{13} & L_{23} & L_{33} & L_{34} \\ L_{14} & L_{24} & L_{34} & L_{44} \end{pmatrix} \begin{pmatrix} -E_M \\ -\partial \ln T_M \\ \partial E_{FE} \\ -\partial \ln T_{FE} \end{pmatrix} \quad (1)$$

where we already inserted the Onsager-Kelvin relation $L_{ij} = L_{ji}$ between the off-diagonal transport coefficients. We focus here on the steady state with finite E_M that induces polarization and heat currents in the ferroelectric. In the following, we disregard small thermoelectric effects in the metal, thermal leakage between the films, and electric field gradients ∂E_{FE} at the edges of the ferroelectric. The task then reduces to the calculation of the polarization drag $\vartheta_D \equiv L_{13}/L_{11}$ as well as the thermoelectric effects summarized by

$$\begin{pmatrix} -j_c \\ j_q^{(FE)} \end{pmatrix} = \begin{pmatrix} L_{11} & L_{14} \\ L_{14} & L_{44} \end{pmatrix} \begin{pmatrix} -E_M \\ -\partial \ln T_{FE} \end{pmatrix} \quad (2)$$

in which we identify the non-local Peltier coefficient $\pi_D = L_{14}/L_{11}$ and thermopower $s_D = \pi_D/T_{FE}$. The electrical conductivity $\sigma = L_{11}$ is also affected by the equilibrium fluctuations of the nearby ferroelectric.

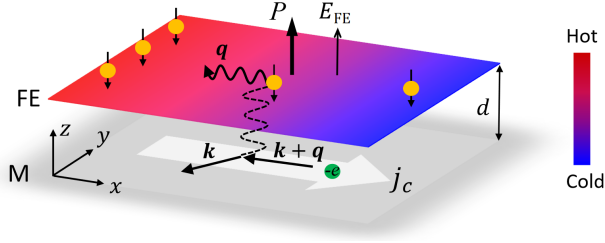


FIG. 1. A schematic of the nonlocal ferra-drag Peltier effect between an extended metallic (M) and a perpendicularly polarized and electrically insulating ferroelectric (FE) film. A charge current (j_c) in the active M sheet transfers its linear momentum to the ferrons in the FE by the electrostatic interaction, leading to heat accumulations at the FE edges. The orange balls represent the ferrons, while the small black arrows are the ferron dipoles that oppose the ferroelectric order and can couple with an out-of-plane electric field (E_{FE}).

The conduction electrons in the metallic layer interact with the electric polarization $\mathbf{P}(\mathbf{r}) = P(\mathbf{r}_{\parallel})\delta(z-d)\hat{\mathbf{z}}$ of the ferroelectric at $z = d$ by the electrostatic energy

$$\mathcal{H}_{\text{int}} = - \int \mathbf{E}_{\text{el}}(\mathbf{r}) \cdot \mathbf{P}(\mathbf{r}) d\mathbf{r}, \quad (3)$$

where

$$\mathbf{E}_{\text{el}}(\mathbf{r}) = - \frac{e}{4\pi\epsilon_r\epsilon_0} \int d\mathbf{r}' \frac{n(\mathbf{r}')}{|\mathbf{r} - \mathbf{r}'|^3} (\mathbf{r} - \mathbf{r}') \quad (4)$$

is the Hartree field of the electrons, $-e$ the electron charge, $n(\mathbf{r}) = n(\mathbf{r}_{\parallel})\delta(z)$ the electron density in the metal at $z = 0$ and ϵ_r the relative permittivity of the separating barrier. Substituting Eq. (4) leads to

$$\mathcal{H}_{\text{int}} = \frac{ed}{4\pi\epsilon_r\epsilon_0} \int \int d\mathbf{r}_{\parallel} d\mathbf{r}'_{\parallel} \frac{P(\mathbf{r}_{\parallel})n(\mathbf{r}'_{\parallel})}{[(\mathbf{r}_{\parallel} - \mathbf{r}'_{\parallel})^2 + d^2]^{3/2}}. \quad (5)$$

where $P(\mathbf{r}_{\parallel})$ and $n(\mathbf{r}_{\parallel})$ represent the 2D polarization and electron density in units of C/m and m^{-2} , respectively.

We model the ferroelectric by the Landau-Ginzburg-Devonshire free energy [33, 34]

$$F = \left(\frac{g}{2} (\nabla P)^2 + \frac{\alpha}{2} P^2 + \frac{\beta}{4} P^4 + \frac{\lambda}{6} P^6 - E_{FE} P \right) \quad (6)$$

where $\alpha = \alpha_0(T - T_c)$, β and $\lambda > 0$ are the Landau coefficients, T_c the Curie-Weiss temperature, $g > 0$ the Ginzburg parameter accounting for the energy cost of an inhomogeneous polarization, and E_{FE} is an out-of-plane electric field acting on the ferroelectric order. The phase transition for $\beta < 0$ ($\beta > 0$) is first (second)-order. A uniform spontaneous polarization P_0 minimizes F by $\alpha P_0 + \beta P_0^3 + \lambda P_0^5 = E_{FE}$, which gives $P_0^2 = [-\beta + (\beta^2 - 4\alpha\lambda)^{1/2}]/(2\lambda)$ when $E_{FE} = 0$. The

non-linear static dielectric susceptibility with the field reads

$$\chi(E_{FE}) = \frac{\partial P_0(E_{FE})}{\partial E_{FE}} = \frac{1}{\alpha + 3\beta P_0^2(E_{FE}) + 5\lambda P_0^4(E_{FE})}. \quad (7)$$

Small fluctuations $\delta P(\mathbf{r}_{\parallel}, t) = P(\mathbf{r}_{\parallel}, t) - P_0$ can be quantized as [24]

$$\delta P(\mathbf{r}_{\parallel}, t) = \sqrt{\frac{\hbar}{2m_p A}} \sum_{\mathbf{q}} \frac{\hat{a}_{\mathbf{q}} e^{i\mathbf{q}\cdot\mathbf{r}_{\parallel}}}{\sqrt{\omega_{\mathbf{q}}}} + \text{H.c.}, \quad (8)$$

where m_p is the polarization inertia that depends on the ionic masses M_i and Born effective charges Q_i in the unit cell of area A_0 as $m_p = A_0(\sum_i Q_i^2/M_i)^{-1}$ [35], A the area of the ferroelectric sheet (assumed to be the same as the metal) and $\hat{a}_{\mathbf{q}}$ ($\hat{a}_{\mathbf{q}}^\dagger$) the annihilation (creation) operator of ferrons with the dispersion relation

$$\omega_{\mathbf{q}} = \left(\frac{gq^2 + \chi(E_{FE})^{-1}}{m_p} \right)^{1/2}. \quad (9)$$

The electric dipole carried by a single ferron is then identified as [24]

$$\delta p_{\mathbf{q}} = - \frac{\partial \hbar \omega_{\mathbf{q}}}{\partial E_{FE}} = \frac{\hbar}{2m_p \omega_{\mathbf{q}}} \frac{\partial \ln \chi}{\partial P_0} < 0 \quad (10)$$

where the negative sign indicates its opposite direction to the ferroelectric order.

In 2D momentum space Eq. (5) now reads

$$\mathcal{H}_{\text{int}} = \frac{e}{2\epsilon_r\epsilon_0 A} \sum_{\mathbf{q}} e^{-d\mathbf{q}} n(\mathbf{q}) \int d\mathbf{r}_{\parallel} \delta P(\mathbf{r}_{\parallel}) e^{i\mathbf{q}\cdot\mathbf{r}_{\parallel}} \quad (11)$$

where we dropped a constant energy shift related to P_0 and $n(\mathbf{q}) = \sum_{\mathbf{k}\nu\nu'} F_{\mathbf{k}\nu}^\dagger F_{(\mathbf{k}+\mathbf{q})\nu'} \hat{c}_{\mathbf{k}\nu}^\dagger \hat{c}_{(\mathbf{k}+\mathbf{q})\nu'}$ is the Fourier component of the 2D electron density in terms of the field operators $\hat{c}_{\mathbf{k}\nu}^\dagger$ and $\hat{c}_{\mathbf{k}\nu}$ with momentum \mathbf{k} , band index ν and the corresponding spinor wave functions $F_{\mathbf{k}\nu}$. $F_{\mathbf{k}'\nu'}^\dagger F_{\mathbf{k}\nu} = (e^{i(\theta_{\mathbf{k}'} - \theta_{\mathbf{k}})} + \nu\nu')/2 = \delta_{\nu,\nu'}$ for graphene (normal metals), where $\tan \theta_{\mathbf{k}} = k_y/k_x$ and $\nu = +1$ and $\nu = -1$ indicate the conduction and valence bands, respectively [36, 37]. Substituting Eq. (8) yields

$$\mathcal{H}_{\text{int}} = \sum_{\mathbf{k}\mathbf{q}\nu\nu'} V_{\mathbf{k}\mathbf{q}}(\nu', \nu) \hat{c}_{(\mathbf{k}+\mathbf{q})\nu'}^\dagger \hat{c}_{\mathbf{k}\nu} \hat{a}_{\mathbf{q}} + \text{H.c.}, \quad (12)$$

where

$$V_{\mathbf{k}\mathbf{q}}(\nu', \nu) = \frac{e}{2\epsilon_r\epsilon_0} \sqrt{\frac{\hbar}{2m_p A}} \frac{e^{-d\mathbf{q}}}{\sqrt{\omega_{\mathbf{q}}}} F_{(\mathbf{k}+\mathbf{q})\nu'}^\dagger F_{\mathbf{k}\nu} \quad (13)$$

is the bare inelastic scattering amplitude of the electrons.

The screening by the conduction electrons and electric dipoles is a many-body problem in which $V_{\mathbf{k}\mathbf{q}}(\nu', \nu) \rightarrow V_{\mathbf{k}\mathbf{q}}(\nu', \nu)/\epsilon(q, \omega)$ and $\epsilon(q, \omega)$ is the dielectric function.

At sufficiently high conduction electron densities, the ferron energies are small compared to the Fermi energy and we may adopt static screening $\omega \rightarrow 0$. For $q < 1/(2d) \lesssim 2k_F$, where k_F is the Fermi wave vector, it is sufficient to adopt the Thomas-Fermi screening approximation [36–41], i.e.,

$$V_{\mathbf{kq}}(\nu', \nu) \rightarrow U_{\mathbf{kq}}(\nu'\nu) = \frac{V_{\mathbf{kq}}(\nu'\nu)}{1 + q_{\text{TF}}/q} \quad (14)$$

where $q_{\text{TF}} = e^2 D_F / (2\epsilon_r \epsilon_0)$ is the 2D Thomas-Fermi wave vector in terms of the density of state D_F at Fermi level. The screening by the ferroelectric dipoles is negligibly small compared to that of the free electrons when the ferroelectric sheet is sufficiently thin. The screening then does not depend on d .

We consider now the effect of a charge current j_c driven by an electric field (E_M) along the x direction in the metallic sheet that deforms the electron distribution function $f_{\mathbf{k}\nu}$ from the Fermi-Dirac form $f_{\mathbf{k}\nu}^{(0)} = [\exp((\varepsilon_{\mathbf{k}\nu} - \varepsilon_F)/k_B T) + 1]^{-1}$ in momentum space, where $\varepsilon_{\mathbf{k}\nu}$ is the electronic band structure, ε_F the Fermi energy, T the temperature, and k_B Boltzmann's constant. Within relaxation time approximation the linearized Boltzmann equation in the metal reads

$$f_{\mathbf{k}\nu} = f_{\mathbf{k}\nu}^{(0)} + e\tau_e v_{\mathbf{k}\nu}^{(x)} E_M \frac{\partial f_{\mathbf{k}\nu}^{(0)}}{\partial \varepsilon_{\mathbf{k}\nu}} \quad (15)$$

where τ_e is the relaxation time and $v_{\mathbf{k}\nu}^{(x)} = \partial \varepsilon_{\mathbf{k}\nu} / \partial \hbar k_x$ the group velocities in transport (x) direction, with $v_{\mathbf{k}\nu}^{(x)} \rightarrow \hbar k_x / m_e$ ($\nu v_F k_x / |\mathbf{k}|$) for a free electron gas with effective mass m_e (or a Dirac cone of graphene with Fermi velocity v_F). The associated electric current density reads $j_c = \sigma E_M$, where

$$\sigma = \frac{e^2 \tau_e \delta}{A} \sum_{\mathbf{k}} (v_{\mathbf{k}\nu}^{(x)})^2 \left(-\frac{\partial f_{\mathbf{k}\nu}^{(0)}}{\partial \varepsilon_{\mathbf{k}\nu}} \right) \quad (16)$$

is the electrical conductivity and δ includes the spin and valley degeneracies.

In the Supplemental Material A [42] we derive a ferron-electron scattering contribution that drastically reduces the τ_e at the Curie temperature of the ferroelectric. The observation of the predicted critical enhancement of the scattering rate would provide a proof of ferron excitations independent of the thermoelectric effects discussed in the following.

The bosonic ferron distribution function $N_{\mathbf{q}}$ in the ferroelectric is governed by another linearized Boltzmann equation [24, 43]. Far from the edges and in the absence of temperature or effective field gradients, the steady state distribution reads

$$N_{\mathbf{q}} = N_{\mathbf{q}}^{(0)} + \tau_f \left. \frac{\partial N_{\mathbf{q}}}{\partial t} \right|_{\text{int}} \quad (17)$$

where $N_{\mathbf{q}}^{(0)} = [\exp(\hbar\omega_{\mathbf{q}}/k_B T) - 1]^{-1}$ is the equilibrium Planck distribution, τ_f the ferron relaxation time. The new ingredient is the collision integral $\partial N_{\mathbf{q}} / \partial t|_{\text{int}}$, which by the current in the metal and via the interlayer interaction $U_{\mathbf{q}}$ renders $N_{\mathbf{q}} \neq N_{-\mathbf{q}}$. The electrons scatter from occupied to empty states, creating and annihilating a ferron in the process. According to Fermi's Golden Rule

$$\left. \frac{\partial N_{\mathbf{q}}}{\partial t} \right|_{\text{int}} = \frac{2\pi\delta}{\hbar} \sum_{\mathbf{k}} |U_{\mathbf{kq}}|^2 [(1 + N_{\mathbf{q}})f_{(\mathbf{k}+\mathbf{q})\nu}(1 - f_{\mathbf{k}\nu}) - N_{\mathbf{q}}f_{\mathbf{k}\nu}(1 - f_{(\mathbf{k}+\mathbf{q})\nu})] \delta(\varepsilon_{\mathbf{k}\nu} - \varepsilon_{(\mathbf{k}+\mathbf{q})\nu} + \hbar\omega_{\mathbf{q}}) \quad (18)$$

while energy and momentum are conserved. Here insignificant interband processes ($\nu \neq \nu'$) have been discarded. To leading order, we may replace $N_{\mathbf{q}}$ on the r.h.s. of Eq. (18) with $N_{\mathbf{q}}^{(0)}$ and substitute the distribution function of the field-biased conductor Eq. (15):

$$N_{\mathbf{q}} = N_{\mathbf{q}}^{(0)} + \frac{2\pi\delta\tau_f}{\hbar} \frac{\partial N_{\mathbf{q}}^{(0)}}{\partial \hbar\omega_{\mathbf{q}}} \sum_{\mathbf{k}} |U_{\mathbf{kq}}|^2 (f_{(\mathbf{k}+\mathbf{q})\nu}^{(0)} - f_{\mathbf{k}\nu}^{(0)}) \times e\tau_e E_M (v_{\mathbf{k}+\mathbf{q}}^{(x)} - v_{\mathbf{k}}^{(x)}) \delta(\varepsilon_{\mathbf{k}\nu} - \varepsilon_{(\mathbf{k}+\mathbf{q})\nu} + \hbar\omega_{\mathbf{q}}). \quad (19)$$

We can now derive the non-local Peltier $\pi_D = -j_q^{(\text{FE})}/j_c$ and polarization drag $\vartheta_D = j_p/j_c$ coefficients by evaluating the heat and polarization currents for the deformed ferron distribution functions by $j_q^{(\text{FE})} = A^{-1} \sum_{\mathbf{q}} u_{\mathbf{q}}^{(x)} N_{\mathbf{q}} \hbar\omega_{\mathbf{q}}$ and $j_p = A^{-1} \sum_{\mathbf{q}} u_{\mathbf{q}}^{(x)} N_{\mathbf{q}} \delta p_{\mathbf{q}}$, respectively, where $u_{\mathbf{q}}^{(x)} = \partial \omega_{\mathbf{q}} / \partial q_x$ is the ferron group velocity along x direction:

$$\begin{aligned} \pi_D &= \frac{2\pi e \tau_f \tau_e \delta}{\sigma \hbar A} \sum_{\mathbf{kq}} \hbar\omega_{\mathbf{q}} u_{\mathbf{q}}^{(x)} (v_{\mathbf{k}+\mathbf{q}}^{(x)} - v_{\mathbf{k}}^{(x)}) \frac{\partial N_{\mathbf{q}}^{(0)}}{\partial \hbar\omega_{\mathbf{q}}} |U_{\mathbf{kq}}|^2 \\ &\quad \times (f_{(\mathbf{k}+\mathbf{q})\nu}^{(0)} - f_{\mathbf{k}\nu}^{(0)}) \delta(\varepsilon_{\mathbf{k}\nu} - \varepsilon_{(\mathbf{k}+\mathbf{q})\nu} + \hbar\omega_{\mathbf{q}}) \quad (20) \\ \vartheta_D &= \frac{2\pi e \tau_f \tau_e \delta}{\sigma \hbar A} \sum_{\mathbf{kq}} \delta p_{\mathbf{q}} u_{\mathbf{q}}^{(x)} (v_{\mathbf{k}+\mathbf{q}}^{(x)} - v_{\mathbf{k}}^{(x)}) \frac{\partial N_{\mathbf{q}}^{(0)}}{\partial \hbar\omega_{\mathbf{q}}} |U_{\mathbf{kq}}|^2 \\ &\quad \times (f_{(\mathbf{k}+\mathbf{q})\nu}^{(0)} - f_{\mathbf{k}\nu}^{(0)}) \delta(\varepsilon_{\mathbf{k}\nu} - \varepsilon_{(\mathbf{k}+\mathbf{q})\nu} + \hbar\omega_{\mathbf{q}}). \quad (21) \end{aligned}$$

We proceed by adopting the quasi-elastic approximation, i.e., $\delta(\varepsilon_{\mathbf{k}\nu} - \varepsilon_{(\mathbf{k}+\mathbf{q})\nu} + \hbar\omega_{\mathbf{q}}) \approx \delta(\varepsilon_{\mathbf{k}\nu} - \varepsilon_{(\mathbf{k}+\mathbf{q})\nu})$, assuming that the Fermi energy is much larger than that of the ferrons ($\lesssim 10$ meV) [24]. This is the case in graphene with homogeneous electron densities $n_0 > 10^{12} \text{ cm}^{-2}$ and Fermi energies $\varepsilon_F > 0.11$ eV [41]. At $k_B T \ll \varepsilon_F$, $f_{\mathbf{k}\nu} - f_{(\mathbf{k}+\mathbf{q})\nu} \simeq \hbar\omega_{\mathbf{q}} \delta(\varepsilon_{\mathbf{k}\nu} - \varepsilon_F)$ and we find

$$\begin{aligned} \pi_D &\simeq \frac{e\tau_f g \hbar^3 D_F^2}{32\delta m_p^2 \varepsilon_0^2 n_0 k_F k_B T} \int_0^{2k_F} \frac{\cos^2(\theta/2) q^2 dq}{\sqrt{1 - (q/2k_F)^2}} \\ &\quad \times \frac{e^{-2dq}}{(1 + q_{\text{TF}}/q)^2} \text{csch}^2 \left(\frac{\hbar\omega_{\mathbf{q}}}{2k_B T} \right). \quad (22) \end{aligned}$$

In contrast to the free electron gas there is a factor $\cos^2(\theta/2)$ that arises from the overlap $|F_{(\mathbf{k}+\mathbf{q})\nu}^\dagger F_{\mathbf{k}\nu}|^2$, where θ is the scattering angle determined by $q = 2k_F \sin(\theta/2)$. A similar expression can be derived for ϑ_D by replacing $\hbar\omega_q$ with δp_q .

The spatial separation limits the momentum transfer exponentially via the factor $\exp(-2dq)$ to $q < 1/(2d)$. At large distances with $k_F d \gg 1$, $q_{\text{TF}} d \gg 1$ and $d \gg l \equiv \sqrt{g\chi}$, only the ferrons located near the center of Brillouin zone contribute and

$$\begin{aligned} \pi_D &\approx \frac{3\pi}{8\delta^2} \frac{\tau_f \omega_0}{(k_F d)^3} \left(\frac{l}{d}\right)^2 \left(\frac{\hbar^2}{e^3 m_p}\right) \xi_0 \text{csch}^2\left(\frac{\xi_0}{2}\right) \\ &\simeq \frac{3\pi}{2\delta^2} \frac{\tau_f \omega_0}{(k_F d)^3} \left(\frac{l}{d}\right)^2 \left(\frac{\hbar^2}{e^3 m_p}\right) \begin{cases} \xi_0 e^{-\xi_0}, & \xi_0 \gg 1 \\ \xi_0^{-1}, & \xi_0 \ll 1 \end{cases} \\ \vartheta_D &\approx \frac{\pi_D}{2} \frac{\partial \chi}{\partial P_0} \end{aligned} \quad (23)$$

where $\xi_0 = \hbar\omega_0/k_B T$ and $\omega_0 = (\chi m_p)^{-1/2}$ the ferron gap. $l \equiv \sqrt{g\chi}$ is the coherence length of the ferroelectric order, a measure of the ferroelectric domain wall width [44, 45]. Since magnetic domain wall widths that scale like $\sim \sqrt{J/K}$, where J is the exchange interaction and K is the anisotropy that governs the magnon gap, χ^{-1} plays the role of the anisotropy by stiffening the ferroelectric order.

The T/d^5 scaling relation at large distances and elevated temperatures for the drag efficiency differs from that of the Coulomb drag effect between two metallic sheets ($\sim T^2/d^4$) [1, 2]. We can trace the difference to the faster decay of electron-dipole interactions ($\sim r^{-2}$) compared to those between charges ($\sim r^{-1}$) as a function of distance while the Planck distribution of the ferrons compared to the Fermi distribution of electrons leads to an increased phase space for scatterings at low temperatures ($k_B T \ll \varepsilon_F$).

For a numerical estimate, we consider here a bilayer composed of graphene and van der Waals ferroelectric monolayer and separated by an inert h-BN layer with (out-of-plane) $\epsilon_r = 3.76$ [46]. In graphene $\varepsilon_{\mathbf{k}\nu} = \nu \hbar v_F |\mathbf{k}|$ with $v_F = 10^8$ cm/s, $D_F = 2\varepsilon_F/(\pi \hbar^2 v_F^2)$, $\delta = 4$ and $k_F = (4\pi n_0/\delta)^{1/2}$ [41]. The parameters for the ferroelectric are adopted as: $\tau_f = 1$ ps, $T_c = 326$ K, $\alpha_0 = 1.54 \times 10^3$ VK $^{-1}$ /pC, $\beta = 1.48 \times 10^5$ Vcm 2 /pC 3 , $\lambda = 2.75 \times 10^4$ Vcm 4 /pC 5 and $g = 0.33$ Vm 2 /C, and $m_p = 10^{-8}$ Vs 2 /C, which are close to those of the monolayer SnSe with in-plane polarization [47]. Figure 2 shows the ferron-drag Peltier coefficient as a function of graphene excess electron density (n_0) for various interlayer distances d at room temperature. π_D has a maximum at an optimal n_0 that decreases with d because a larger n_0 increases the electron-ferron scattering for small n_0 while the increased screening wins at larger densities, which is easier for larger d . π_D depends not only on the

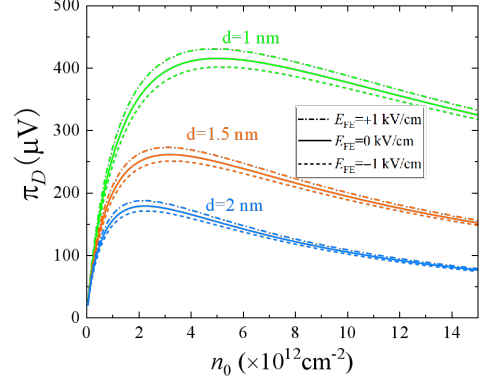


FIG. 2. The nonlocal ferron-drag Peltier coefficient (π_D) as a function of the electron concentration (n_0) in graphene for various interlayer distance (d). The π_D exhibit an asymmetric dependence on the relative direction of an external field (E_{FE}) to the ferroelectric order.

strength, but also on the direction of an external electric field (below the coercive field), i.e., π_D is reduced (enhanced) by the positive (negative) field along the ferroelectric order, because of the fact that the ferrons carry nonzero electric dipoles.

The drag effect results in heat and polarization accumulations in the ferroelectric (see figure 1). Assuming that both films are thermally isolated, a temperature gradient $T_{\text{FE}}(x) = T_0 + \partial T_{\text{FE}}(x - L/2)$ emerges in a ferroelectric with length L , where T_0 is the ambient temperature. The open circuit condition for the heat current, i.e., $j_q^{(\text{FE})} = -\pi_D j_c - \kappa_{\text{FE}} \partial T_{\text{FE}} = 0$, leads to $\partial T_{\text{FE}} = (-\pi_D/\kappa_{\text{FE}}) j_c$, where κ_{FE} is the 2D thermal conductivity of the ferroelectric sheet (in units of W/K). The polarization accumulation $\Delta P(x)$ vanishes except for the neighborhood of the edges on the scale of the polarization relaxation length [22].

With $d = 1$ nm, $n_0 = 10^{13}$ cm $^{-2}$, we have $\pi_D = 367$ μV at the room temperature. The maximum current density in graphene is limited by self-heating to ~ 30 A/cm [48], but even for $j_c = 3.4 \times 10^{-2}$ A/cm (or a bulk current density $j_c^{(b)} = 10^6$ A/cm 2) this modest Peltier coefficient generates a large temperature gradient $\partial T_{\text{FE}} = 5$ K/ μm for $\kappa_{\text{FE}} = 2.5 \times 10^{-10}$ W/K (or bulk $\kappa_{\text{FE}}^{(b)} = 0.5$ W/Km for a monolayer thickness of 5 \AA [49]) because of the simultaneous low thermal conductivity of the ferroelectric and high available current density in graphene. This should be easily observable close to the edges, even when some heat current leaks from the ferroelectric into the graphene. Inversely, a temperature gradient in the ferroelectric generates a charge current in graphene, i.e., a nonlocal ferron-drag thermopower. $s_D = \pi_D/T_0 = 1.23$ $\mu\text{V}/\text{K}$ at $T_0 = 298$ K. However, this number is at least an order of magnitude smaller than that of a single graphene

[50, 51].

For sufficient thermal isolation between the ferroelectric and graphene layers the figure of merit of the ferron drag thermoelectric device can be defined and estimated as

$$(ZT)_D = \frac{\sigma s_D^2 T_0}{\kappa_{FE}} = 2.6 \times 10^{-3} \quad (24)$$

where $\sigma = 1.38 \times 10^{-3}$ S is the electrical conductivity with the nearby ferroelectric at $n_0 = 10^{13} \text{ cm}^{-2}$ [42]. This $(ZT)_D$ is comparable to that of graphene [52] but it may be engineered to become larger by, e.g., optimizing the electron density of graphene as shown in figure 2 or stacking m ferroelectric monolayers with $(ZT)_D \propto m$ as long as all of them stay in the range of the dipolar interaction. The predicted substantial FOM in spite of the small s_D relies on beating the Wiedemann-Franz Law that hinders conventional thermoelectric devices: The small heat conductivity in the ferroelectric does not depend on the electric conductivity in the conductor, which is large in graphene in spite of the additional ferron scattering [42].

According to Supplemental Material B [42] the current drag is not specific for ferrons: the expressions are identical for in-plane longitudinal and out-of-plane polarized polar optical phonons, except for the difference in the frequency dispersions and other relevant parameters. We therefore encourage search for thermoelectric effects in any highly polarizable insulator. The attraction of using ferroelectrics is strong dependence and control of larger effects by temperature and applied electric field as well as non-volatile switching of the ferroelectric order. The critical enhancement of the electrical resistance at the Curie temperature is also unique for ferroelectrics.

Conclusion: We predict significant non-local ferron-drag thermoelectric effects in bilayers of ferroelectric insulators and conductors that are separated by a small distance d . A remote gate-field controlled Peltier effect can be detected by standard thermography and would prove the existence of the ferron quasiparticles in ferroelectrics. The results can be readily extended to the limit $d = 0$ corresponding to van der Waals conducting ferroelectrics, known as ferroelectric metals, in which electric polarization and mobile electrons coexist [53], and the ferroelectrics with in-plane spontaneous polarization. In the dipole approximation of the ferroelectric charge dynamics, the mobile electrons cannot screen the perpendicular ferroelectric order nor couple to the longitudinal ferrons. We may expect a strong coupling to the transverse ferrons, however, with associated interesting thermoelectric phenomena presently under investigation. Our work opens a new strategy for the design of thermoelectric devices that are not bound by the Wiedemann-Franz Law.

Acknowledgements: We acknowledge the helpful discussions with Ryo Iguchi. JSPS KAKENHI Grant No. 19H00645 supported P.T. and G.B and Grant No.

22H04965 supported G.B. and K.U. K.U. also acknowledges support by JSPS KAKENHI Grant No. 20H02609 and JST CREST “Creation of Innovative Core Technologies for Nano-enabled Thermal Management” Grant No. JPMJCR17I1.

-
- [1] T. J. Gramila, J. P. Eisenstein, A. H. MacDonald, L. N. Pfeiffer, and K. W. West, Mutual Friction between Parallel Two-Dimensional Electron Systems, *Phys. Rev. Lett.* **66**, 1216 (1991).
 - [2] A. Jauho and H. Smith, Coulomb drag between parallel two-dimensional electron systems, *Phys. Rev. B* **47**, 4420 (1993).
 - [3] B. Narozhny and A. Levchenko, Coulomb drag, *Rev. Mod. Phys.* **88**, 025003 (2016).
 - [4] M. Bailyn, Phonon-drag part of the thermoelectric power in metals, *Phys. Rev.* **157**, 480 (1967).
 - [5] D. Cantrell and P. Butcher, A calculation of the phonon-drag contribution to the thermopower of quasi-2D electrons coupled to 3D phonons, *Journal of Physics C: Solid State Physics* **20**, 1985 (1987).
 - [6] S. Lyo, Low-temperature phonon-drag thermoelectric power in heterojunctions, *Phys. Rev. B* **38**, 6345(R) (1988).
 - [7] J. Vavro, M. C. Llaguno, J. E. Fischer, S. Ramesh, R. K. Saini, L. M. Ericson, V. A. Davis, R. H. Hauge, M. Pasquali, and R. E. Smalley, Thermoelectric Power of p-Doped Single-Wall Carbon Nanotubes and the Role of Phonon Drag, *Phys. Rev. Lett.* **90**, 065503 (2003).
 - [8] H. C. Tso, P. Vasilopoulos, and F. M. Peeters, Direct Coulomb and phonon-mediated coupling between spatially separated electron gases, *Phys. Rev. Lett.* **68**, 2516 (1992).
 - [9] M. C. Bønsager, K. Flensberg, B. Y. Hu, and A. H. MacDonald, Frictional drag between quantum wells mediated by phonon exchange, *Phys. Rev. B* **57**, 7085 (1998).
 - [10] H. Noh, S. Zelakiewicz, T. J. Gramila, L. N. Pfeiffer, and K. W. West, Phonon-mediated drag in double-layer two-dimensional electron systems, *Phys. Rev. B* **59**, 13114 (1999).
 - [11] M. Bailyn, Maximum Variational Principle for Conduction Problems in a Magnetic Field, and the Theory of Magnon Drag, *Phys. Rev.* **126**, 2040 (1962).
 - [12] F. Blatt, D. Flood, V. Rowe, P. Schroeder, and J. Cox, Magnon-Drag Thermopower in Iron, *Phys. Rev. Lett.* **18**, 395 (1967).
 - [13] G. N. Grannemann and L. Berger, Magnon-drag Peltier effect in a Ni-Cu alloy, *Phys. Rev. B* **13**, 2072 (1976).
 - [14] M. V. Costache, G. Bridoux, I. Neumann and S. O. Valenzuela, Magnon-drag thermopile, *Nat. Mater.* **11**, 199 (2012).
 - [15] B. Flebus, R. A. Duine, and Y. Tserkovnyak, Landau-Lifshitz theory of the magnon-drag thermopower, *Europhys. Lett.* **115**, 57004 (2016).
 - [16] S. J. Watzman, R. A. Duine, Y. Tserkovnyak, S. R. Boona, H. Jin, A. Prakash, Y. Zheng, and J. P. Heremans, Magnon-drag thermopower and Nernst coefficient in Fe, Co, and Ni, *Phys. Rev. B* **94**, 144407 (2016).
 - [17] S. S.-L. Zhang and S. Zhang, Magnon Mediated Electric Current Drag Across a Ferromagnetic Insulator Layer,

- Phys. Rev. Lett. **109**, 096603 (2012).
- [18] H. Wu, C. H. Wan, X. Zhang, Z. H. Yuan, Q. T. Zhang, J. Y. Qin, H. X. Wei, X. F. Han, and S. Zhang, Observation of magnon-mediated electric current drag at room temperature, Phys. Rev. B **93**, 060403(R) (2016).
- [19] J. Li, Y. Xu, M. Aldosary, C. Tang, Z. Lin, S. Zhang, R. Lake, and J. Shi, Observation of magnon-mediated current drag in Pt/yttrium iron garnet/Pt(Ta) trilayers, Nat. Commun. **7**, 10858 (2016).
- [20] T. Liu, G. Vignale, and M. E. Flatté, Nonlocal Drag of Magnons in a Ferromagnetic Bilayer, Phys. Rev. Lett. **116**, 237202 (2016).
- [21] Y. Kainuma, R. Iguchi, D. Prananto, V. I. Vasyuchka, B. Hillebrands, T. An, and K. Uchida, Local heat emission due to unidirectional spin-wave heat conveyer effect observed by lock-in thermography, Appl. Phys. Lett. **118**, 222404 (2021).
- [22] G. E. W. Bauer, R. Iguchi, and K. Uchida, Theory of transport in ferroelectric capacitors, Phys. Rev. Lett. **126**, 187603 (2021).
- [23] P. Tang, R. Iguchi, K. Uchida, G. E. W. Bauer, Thermoelectric Polarization Transport in Ferroelectric Ballistic Point Contacts, Phys. Rev. Lett. **128**, 047601 (2022).
- [24] P. Tang, R. Iguchi, K. Uchida, Gerrit E. W. Bauer, Excitations of the ferroelectric order, [arXiv:2203.06367](https://arxiv.org/abs/2203.06367) (2022).
- [25] K. Chang, J. Liu, H. Lin, N. Wang, K. Zhao, A. Zhang, F. Jin, Y. Zhong, X. Hu, W. Duan, Q. Zhang, L. Fu, Qi-Kun Xue, X. Chen, and Shuai-Hua Ji, Discovery of robust in-plane ferroelectricity in atomic-thick SnTe, Science **353**, 274 (2016).
- [26] F. Liu, L. You, K. L. Seyler, X. Li, P. Yu, J. Lin, X. Wang, J. Zhou, H. Wang, H. He, S. T. Pantelides, W. Zhou, P. Sharma, X. Xu, P. M. Ajayan, J. Wang, and Z. Liu, Room-temperature ferroelectricity in CuInP₂S₂ ultrathin flakes. Nat. Commun. **7**, 12357 (2016).
- [27] L. Li and M. Wu, Binary compound bilayer and multilayer with vertical polarizations: Two-dimensional ferroelectrics, multiferroics, and nanogenerators, ACS Nano **11**, 6382 (2017).
- [28] Q. Yang, M. Wu, and J. Li, Origin of two-dimensional vertical ferroelectricity in WTe₂ bilayer and multilayer, J. Phys. Chem. Lett. **9**, 7160 (2018).
- [29] Z. Fei, W. Zhao, T. A. Palomaki, B. Sun, M. K. Miller, Z. Zhao, J. Yan, X. Xu, and D. H. Cobden, Ferroelectric switching of a two-dimensional metal, Nature **560**, 336 (2018).
- [30] S. Yuan, X. Luo, H. L. Chan, C. Xiao, Y. Dai, M. Xie, and J. Hao, Room-temperature ferroelectricity in MoTe₂ down to the atomic monolayer limit, Nat. Commun. **10**, 1775 (2019).
- [31] K. Yasuda, X. Wang, K. Watanabe, T. Taniguchi, P. Jarillo-Herrero, Stacking-engineered ferroelectricity in bilayer boron nitride, Science **372**, 1458 (2021).
- [32] X. Wang, K. Yasuda, Y. Zhang, S. Liu, K. Watanabe, T. Taniguchi, J. Hone, L. Fu, and P. Jarillo-Herrero, Interfacial ferroelectricity in rhombohedral-stacked bilayer transition metal dichalcogenides. Nat. Nanotechnol. **17**, 367 (2022).
- [33] A. F. Devonshire, Theory of barium titanate: Part I, The London, Edinburgh, and Dublin Philosophical Magazine and Journal of Science **40**, 1040 (1949).
- [34] A. Devonshire, Theory of barium titanate: Part II, The London, Edinburgh, and Dublin Philosophical Magazine and Journal of Science **42**, 1065 (1951).
- [35] S. Sivasubramanian, A. Widom, and Y. N. Srivastava, Physical kinetics of ferroelectric hysteresis, Ferroelectrics **300**, 43 (2004).
- [36] T. Ando, Screening Effect and Impurity Scattering in Monolayer Graphene, J. Phys. Soc. Jpn. **75**, 074716 (2006).
- [37] E. H. Hwang and S. D. Sarma, Screening-induced temperature-dependent transport in two-dimensional graphene, Phys. Rev. B **79**, 165404 (2009).
- [38] F. Stern, Polarizability of a Two-Dimensional Electron Gas, Phys. Rev. Lett. **18**, 546 (1967).
- [39] T. Ando, A. B. Fowler, and F. Stern, Electronic properties of two-dimensional systems, Rev. Mod. Phys. **54**, 437 (1982).
- [40] E. H. Hwang and S. Das Sarma, Dielectric function, screening, and plasmons in two-dimensional graphene, Phys. Rev. B **75**, 205418 (2007).
- [41] S. D. Sarma, S. Adam, E. H. Hwang, and E. Rossi, Electronic transport in two-dimensional graphene, Rev. Mod. Phys. **83**, 407 (2011).
- [42] See the Supplemental Material for the influence of ferron-electron scatterings on the electrical conductivity in the metal and the drag effect of in-plane polarization fluctuations (polar optical phonons).
- [43] G. E. W. Bauer, P. Tang, R. Iguchi, K. Uchida, Magnonics vs. Ferronics, J. Magn. Magn. Mater. **541**, 168468 (2022).
- [44] Y. Ishibashi, Phenomenological theory of domain walls, Ferroelectrics **98**, 193 (1989).
- [45] Y. Ishibashi, Structure and physical properties of domain walls, Ferroelectrics **104**, 299 (1990).
- [46] A. Laturia, M.L. van de Put, W.G. Vandenberghe, Dielectric properties of hexagonal boron nitride and transition metal dichalcogenides: from monolayer to bulk. npj 2D Mater Appl **2**, 6 (2018).
- [47] R. Fei, W. Kang, and L. Yang, Ferroelectricity and Phase Transitions in Monolayer Group-IV Monochalcogenides, Phys. Rev. Lett. **117**, 097601 (2016).
- [48] A. D. Liao, J. Z. Wu, X. Wang, K. Tahy, D. Jena, H. Dai, and E. Pop, Thermally Limited Current Carrying Ability of Graphene Nanoribbons, Phys. Rev. Lett. **106**, 256801 (2011).
- [49] C. Li, J. Hong, A. May, D. Bansal, S. Chi, T. Hong, G. Ehlers, and O. Delaire, Ultralow thermal conductivity and high thermoelectric figure of merit in SnSe crystals, Nat. Phys. **11**, 1063 (2015).
- [50] Y. M. Zuev, W. Chang, and P. Kim, Thermoelectric and Magnetothermoelectric Transport Measurements of Graphene, Phys. Rev. Lett. **102**, 096807 (2009).
- [51] P. Wei, W. Bao, Y. Pu, C. N. Lau, and J. Shi, Anomalous Thermoelectric Transport of Dirac Particles in Graphene, Phys. Rev. Lett. **102**, 166808 (2009).
- [52] A. H. Reshak, S. A. Khan and S. Auluck, Thermoelectric properties of a single graphene sheet and its derivatives, J. Mater. Chem. C **2**, 2346 (2014).
- [53] W. X. Zhou and A. Ariando, Review on ferroelectric/polar metals, Jpn. J. Appl. Phys. **59**, SI0802 (2020).

Supplementary Material to “Nonlocal Drag Thermoelectricity Generated by a Ferroelectric Heterostructures”

Ping Tang¹, Ken-ichi Uchida^{2,3}, and Gerrit E. W. Bauer^{1,3,4,5,6}

¹WPI-AIMR, Tohoku University, 2-1-1 Katahira, Sendai 980-8577, Japan

²National Institute for Materials Science, Tsukuba 305-0047, Japan

³Institute for Materials Research, Tohoku University, 2-1-1 Katahira, Sendai 980-8577, Japan

⁴Center for Spintronics Research Network, Tohoku University, Sendai 980-8577, Japan

⁵Zernike Institute for Advanced Materials, University of Groningen, 9747 AG Groningen, Netherlands and

⁶Kavli Institute for Theoretical Sciences, University of the Chinese Academy of Sciences, Beijing 10090, China

In this Supplementary Material, we derive the effect of feron-electron scatterings on the electrical conductivity in the 2D metal (graphene) (Section A) and the current drag on normal polar phonons in ferroelectrics or polar dielectrics (Section B).

A. FERRON FLUCTUATIONS AND ELECTRICAL CONDUCTIVITY OF A NEARBY METAL FILM

The linearized Boltzmann equation within relaxation time approximation for the distribution function $f_{\mathbf{k}\nu}$ in the metal reads

$$eE_M v_{\mathbf{k}\nu}^{(x)} \left(-\frac{\partial f_{\mathbf{k}\nu}^{(0)}}{\partial \varepsilon_{\mathbf{k}\nu}} \right) = -\frac{f_{\mathbf{k}\nu} - f_{\mathbf{k}\nu}^{(0)}}{\tau_e} + \left(\frac{\partial f_{\mathbf{k}\nu}}{\partial t} \right)_{\text{int}} \quad (\text{S.A1})$$

where E_M is the driving field in the x -direction, $v_{\mathbf{k}\nu}^{(x)} = \partial \varepsilon_{\mathbf{k}\nu} / \partial (\hbar k_x)$ the corresponding group velocity, $f_{\mathbf{k}\nu}^{(0)}$ the Fermi-Dirac distribution, τ_e the relaxation time caused by, e.g., impurities, phonons, etc. within the graphene and the second collision term on the right hand side stems from the electron-ferion interactions. Fermi's Golden Rule

$$\begin{aligned} \left(\frac{\partial f_{\mathbf{k}\nu}}{\partial t} \right)_{\text{int}} &= \frac{2\pi}{\hbar} \sum_{\mathbf{q}} |U_{\mathbf{k}\mathbf{q}}|^2 \{ f_{(\mathbf{k}+\mathbf{q})\nu} (1 - f_{\mathbf{k}\nu}) (N_{\mathbf{q}} + 1) - f_{\mathbf{k}\nu} (1 - f_{(\mathbf{k}+\mathbf{q})\nu}) N_{\mathbf{q}} \} \delta(\varepsilon_{\mathbf{k}\nu} + \hbar\omega_{\mathbf{q}} - \varepsilon_{(\mathbf{k}+\mathbf{q})\nu}) \\ &+ \frac{2\pi}{\hbar} \sum_{\mathbf{q}} |U_{\mathbf{k}\mathbf{q}}|^2 \{ f_{(\mathbf{k}-\mathbf{q})\nu} (1 - f_{\mathbf{k}\nu}) N_{\mathbf{q}} - f_{\mathbf{k}\nu} (1 - f_{(\mathbf{k}-\mathbf{q})\nu}) (N_{\mathbf{q}} + 1) \} \delta(\varepsilon_{\mathbf{k}\nu} - \varepsilon_{(\mathbf{k}-\mathbf{q})\nu} - \hbar\omega_{\mathbf{q}}) \end{aligned} \quad (\text{S.A2})$$

includes out-scattering (self-energy) and in-scattering (vertex correction) terms during both the creation and annihilation processes of ferrons. As in the main text, the interband scatterings ($\nu \neq \nu'$) have been discarded again. $N_{\mathbf{q}}$ is the feron distribution in the neighboring ferroelectric layer. We expand the distribution

$$f_{\mathbf{k}\nu} = f_{\mathbf{k}\nu}^{(0)} + \left(-\frac{\partial f_{\mathbf{k}\nu}^{(0)}}{\partial \varepsilon_{\mathbf{k}\nu}} \right) g_{\mathbf{k}\nu} = f_{\mathbf{k}\nu}^{(0)} + \frac{g_{\mathbf{k}\nu}}{k_B T} \left(1 - f_{\mathbf{k}\nu}^{(0)} \right) f_{\mathbf{k}\nu}^{(0)} \quad (\text{S.A3})$$

where $g_{\mathbf{k}\nu}$ represents the nonequilibrium part. In linear response, we replace the feron distribution by the equilibrium Planck distribution $N_q^{(0)}$ and substitute Eq. (S.A3) into Eq. (S.A2), i.e.,

$$\begin{aligned} \left(\frac{\partial f_{\mathbf{k}\nu}}{\partial t} \right)_{\text{int}} &= \frac{2\pi}{\hbar k_B T} \sum_{\mathbf{q}} |U_{\mathbf{k}\mathbf{q}}|^2 (1 - f_{(\mathbf{k}+\mathbf{q})\nu}^{(0)}) f_{\mathbf{k}\nu}^{(0)} N_q^{(0)} [g_{(\mathbf{k}+\mathbf{q})\nu} - g_{\mathbf{k}\nu}] \delta(\varepsilon_{\mathbf{k}\nu} + \hbar\omega_{\mathbf{q}} - \varepsilon_{(\mathbf{k}+\mathbf{q})\nu}) \\ &+ \frac{2\pi}{\hbar k_B T} \sum_{\mathbf{q}} |U_{\mathbf{k}\mathbf{q}}|^2 (1 - f_{\mathbf{k}\nu}^{(0)}) f_{(\mathbf{k}-\mathbf{q})\nu}^{(0)} N_q^{(0)} [g_{(\mathbf{k}-\mathbf{q})\nu} - g_{\mathbf{k}\nu}] \delta(\varepsilon_{\mathbf{k}\nu} - \varepsilon_{(\mathbf{k}-\mathbf{q})\nu} - \hbar\omega_{\mathbf{q}}). \end{aligned} \quad (\text{S.A4})$$

For a uniform charge transport the nonequilibrium part can be written as $g_{\mathbf{k}\nu} = g_{k\nu} \cos \vartheta_{\mathbf{k}}$, where ϑ_k is the angle between an applied field and wave vector, i.e., a Fermi distribution shifted in momentum space. As in the main text, we invoke the quasi-elastic scattering approximation $\delta(\varepsilon_{\mathbf{k}\nu} - \varepsilon_{(\mathbf{k}\pm\mathbf{q})\nu} \pm \hbar\omega_{\mathbf{q}}) \approx \delta(\varepsilon_{\mathbf{k}\nu} - \varepsilon_{(\mathbf{k}\pm\mathbf{q})\nu}) = g_{\mathbf{k}\nu} (\cos \theta_{\mathbf{k}, \mathbf{k}\pm\mathbf{q}} - 1)$ for an isotropic electronic band, and find

$$\left(\frac{\partial f_{\mathbf{k}\nu}}{\partial t} \right)_{\text{int}} \approx -\frac{f_{\mathbf{k}\nu} - f_{\mathbf{k}\nu}^{(0)}}{\tau_D} \quad (\text{S.A5})$$

where

$$\tau_D^{-1} = -\frac{2\pi}{\hbar} \sum_{\mathbf{q}} |U_{\mathbf{kq}}|^2 2\hbar\omega_{\mathbf{q}} \frac{\partial N_q^{(0)}}{\partial \hbar\omega_q} (1 - \cos\theta) \delta(\varepsilon_{\mathbf{k}\nu} - \varepsilon_{(\mathbf{k}+\mathbf{q})\nu}) \quad (\text{S.A6})$$

is the ferron scattering rate and $\theta = \theta_{\mathbf{k},\mathbf{k}+\mathbf{q}}$ the angle between \mathbf{k} and $\mathbf{k} + \mathbf{q}$. Substituting Eq. (S.A6) into Eq. (S.A1) leads to

$$f_{\mathbf{k}\nu} = f_{\mathbf{k}\nu}^{(0)} + e\tilde{\tau}_e v_{\mathbf{k}\nu}^{(x)} E_M \frac{\partial f_{\mathbf{k}\nu}^{(0)}}{\partial \varepsilon_{\mathbf{k}\nu}} \quad (\text{S.A7})$$

where $\tilde{\tau}_e = (\tau_e^{-1} + \tau_D^{-1})^{-1}$ is the effective transport relaxation time. Substituting $U_{\mathbf{kq}}$ from the main text, we find for the graphene

$$\tau_D^{-1} = -\frac{e^2}{16\pi m_p \epsilon_r \epsilon_0^2} \int d^2q \frac{e^{-2dq}}{(1 + q_{\text{TF}}/q)^2} \frac{\partial N_q}{\partial \omega_q} (1 - \cos^2\theta) \delta(\varepsilon_{\mathbf{k}} - \varepsilon_{\mathbf{k}+\mathbf{q}}) \quad (\text{S.A8})$$

where $q = 2k \sin(\theta/2)$.

The exponent limits the momentum transfer to $q < 1/(2d)$. For the electrons at Fermi level with $q_{\text{TF}}d \gg 1$, $k_F d \gg 1$ and $d \gg l$, where $l = \sqrt{g\chi}$ is the ferroelectric coherence length and χ the susceptibility,

$$\tau_D^{-1} \simeq \frac{3\omega_0}{128\pi(k_F d)^2 (q_{\text{TF}} d)^2 (q_c d)} \frac{\hbar\omega_0}{k_B T} \text{csch}^2 \left(\frac{\hbar\omega_0}{2k_B T} \right) \quad (\text{S.A9})$$

with

$$q_c^{-1} = \frac{\chi e^2}{v_F \epsilon_r \epsilon_0^2 \hbar}. \quad (\text{S.A10})$$

At the Curie temperature where $\chi \rightarrow \infty$ and $l \rightarrow \infty$, such that $d \ll l$, we have to reintroduce the ferron dispersion

$$\omega_q = \sqrt{\frac{gq^2 + \chi^{-1}}{m_p}} \approx \sqrt{\frac{g}{m_p}} q. \quad (\text{S.A11})$$

When $k_B T \gg (\hbar/d)\sqrt{g/m_p}$ the Eq. (S.A8) becomes

$$\tau_D^{-1} \simeq \frac{1}{32\pi(k_F d)(q_{\text{TF}} d)^2} \frac{k_B T}{\varepsilon_F} \frac{e^2}{\hbar g \epsilon_r \epsilon_0^2} \quad (\text{S.A12})$$

which is similar to the scattering of electrons by the acoustic phonons in graphene but with different dependence on the carrier density of graphene [1]. The electrical current density is given by

$$j_c = -\frac{4e}{A} \sum_{\mathbf{k}} v_{\mathbf{k}\nu}^{(x)} f_{\mathbf{k}\nu} \quad (\text{S.A13})$$

where the spin and valley degeneracies have been included. Substituting Eq. (S.A7), we arrive at the series resistor model

$$\frac{1}{\sigma} = \frac{1}{\sigma_0} + \frac{1}{\sigma_D} \quad (\text{S.A14})$$

where $\sigma_0 \simeq e^2 v_F^2 \tau_e D_F / 2$ and $\sigma_D \simeq e^2 v_F^2 \tau_D D_F / 2$.

In Fig. S1 we show a plot of τ_D^{-1} (at the Fermi level) and σ_D obtained by computing Eq. (S.A8) as a function of (a) temperature and (b) carrier density n_0 for the parameters used in the main text and different interlayer distances. The τ_D^{-1} (σ_D) is critically enhanced (suppressed) at the Curie temperature (T_c) determined by Eq. (S.A12) and σ_D increases rapidly with n_0 , in sharp contrast to the conductivity limited by the acoustic phonon scattering in graphene [1]. While s_D varies non-monotonically with n_0 (see the main text), the drag power factor defined as $\sigma_D s_D^2$ and shown in (c) is proportional to n_0 .

At room temperature the acoustic phonon scattering limits σ_0 to $\sim 10^{-2}$ S in high-quality graphene [1], so $\sigma \approx \sigma_D = 1.38 \times 10^{-3}$ S and $\sigma s_D^2 \approx 2.21 \times 10^{-3}$ pW/K² for $n_0 = 10^{13}$ cm⁻² used in the main text.

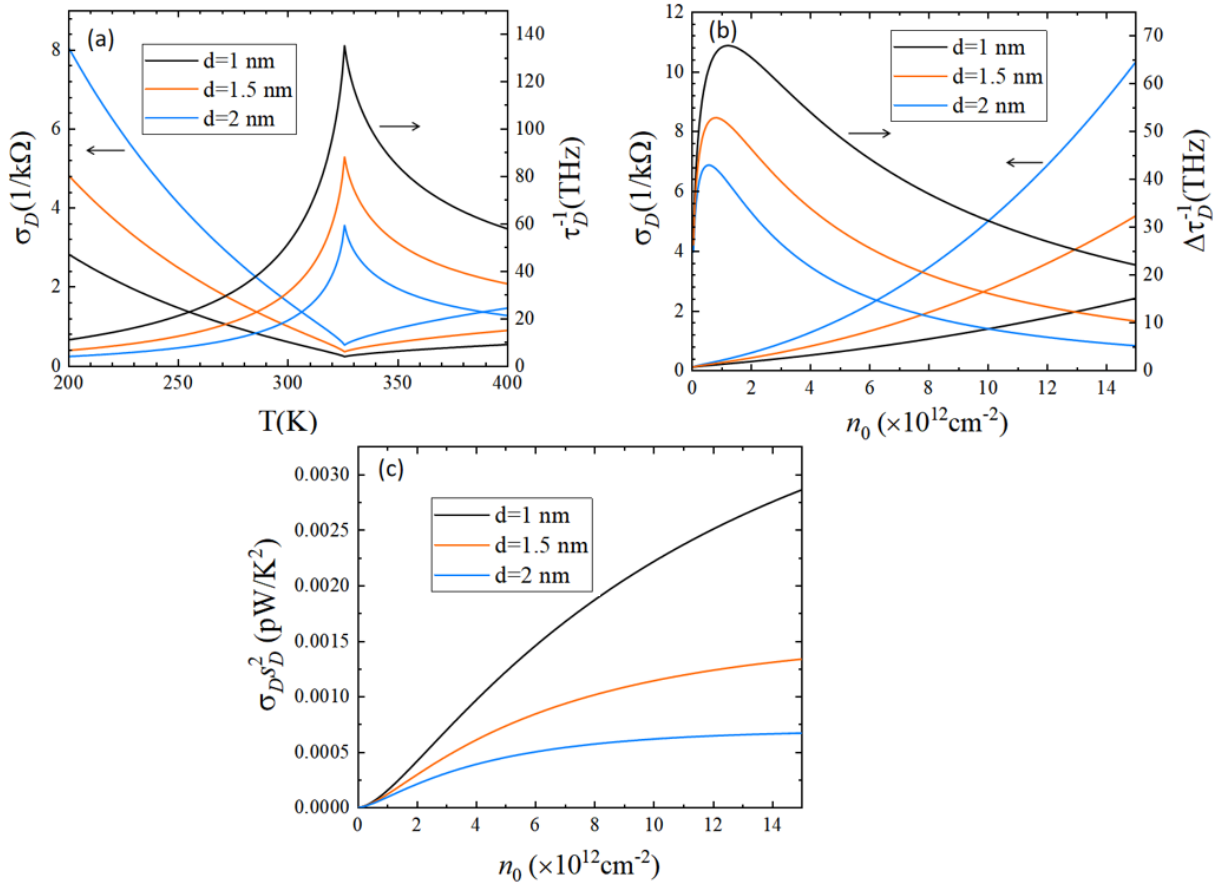


FIG. S1. The scattering rate τ_D^{-1} at the Fermi level and conductivity σ_D of graphene as a function of (a) temperature at a fixed $n_0 = 5 \times 10^{12} \text{ cm}^{-2}$ and (b) carrier density (n_0) at room temperature for several distances to a ferroelectric layer with Curie temperature indicated by the vertical dotted line. (c) The drag power factor $\sigma_D s_D^2$ as a function of n_0 at room temperature.

B. DRAG EFFECT BY POLAR OPTICAL PHONONS

In both ferroelectrics and dielectrics conventional polar optical phonons do not carry net electric dipoles, but still cause harmonic polarization fluctuations $\delta\mathbf{P}$ and bound charges $-\nabla \cdot \delta\mathbf{P}$ that interact with a proximity metal with electron density $n(\mathbf{r})$ by

$$\mathcal{H}_{\text{int}} = \frac{e}{4\pi\epsilon_r\epsilon_0} \int d\mathbf{r} \int d\mathbf{r}' \frac{n(\mathbf{r})\nabla \cdot \delta\mathbf{P}(\mathbf{r}')}{|\mathbf{r} - \mathbf{r}'|} \quad (\text{S.B1})$$

where $e > 0$. To be specific we focus on in-plane polarizations ($\delta\mathbf{P}_{\parallel}$) below, since the treatment of out-of-plane fluctuations is the same as in the main text. The free energy cost by such fluctuations can be modeled by

$$\delta F = \frac{1}{2} \int d\mathbf{r}_{\parallel} \left(g_{\parallel} (\nabla \delta\mathbf{P}_{\parallel})^2 + \alpha_{\parallel} (\delta\mathbf{P}_{\parallel})^2 - \mathbf{E}_{\text{dip}} \cdot \delta\mathbf{P}_{\parallel} \right) \quad (\text{S.B2})$$

where g_{\parallel} (α_{\parallel}) accounts for the energy cost by non-uniform (uniform) fluctuations and \mathbf{E}_{dip} the dipolar electric field associated with the fluctuations. Note that there is no in-plane spontaneous polarization except fluctuations. The $\delta\mathbf{P}_{\parallel}$ are composed of longitudinal and transverse modes with wave vector parallel and perpendicular to their fluctuating directions, respectively. In second quantization,

$$\delta\mathbf{P}_{\parallel} = \sqrt{\frac{\hbar}{2m_p^{\parallel}A}} \sum_{\mathbf{q}, \sigma=L,T} \frac{\mathbf{e}_{\mathbf{q}\sigma}}{\sqrt{\omega_{\mathbf{q}\sigma}}} a_{\mathbf{q}\sigma} e^{i\mathbf{q}\cdot\mathbf{r}} + \text{h.c.} \quad (\text{S.B3})$$

where m_p^\parallel is the inertia of $\delta\mathbf{P}_\parallel$, $\mathbf{e}_{\mathbf{q}\sigma}$ the polarization of polar phonons with the creation operator of $a_{\mathbf{q}\sigma}$ and $\sigma = L, T$ represents the longitudinal ($\mathbf{q} \parallel \mathbf{e}_{\mathbf{q}L}$) and transverse ($\mathbf{q} \perp \mathbf{e}_{\mathbf{q}T}$) polar optical phonon modes. In contrast, the ferron modes (out-of-plane fluctuations) that we label $\omega_{\mathbf{q}}$ are always polarized normal to the plane (wave vector). For the transverse mode, $\nabla \cdot \delta\mathbf{P}_\parallel = 0$, such that $\mathbf{E}_{dip} = 0$, and its dispersion relation is thus given by

$$\omega_{\mathbf{q}T} = \sqrt{\frac{\alpha_\parallel + g_\parallel \mathbf{q}^2}{m_p^\parallel}}. \quad (\text{S.B4})$$

The longitudinal mode carries nonzero $\nabla \cdot \delta\mathbf{P}_\parallel$, which leads to

$$\mathbf{E}_{dip}(\mathbf{r}_\parallel) = -\frac{1}{4\pi\epsilon_r\epsilon_0} \int d\mathbf{r}'_\parallel \frac{\nabla \cdot \delta\mathbf{P}_\parallel(\mathbf{r}'_\parallel)}{|\mathbf{r}_\parallel - \mathbf{r}'_\parallel|^2} \quad (\text{S.B5})$$

and the electrostatic energy

$$-\frac{1}{2} \int d\mathbf{r}_\parallel \mathbf{E}_{dip} \cdot \delta\mathbf{P}_\parallel = \frac{1}{8\pi\epsilon_r\epsilon_0} \int d\mathbf{r}_\parallel \int d\mathbf{r}'_\parallel \frac{\nabla \cdot \delta\mathbf{P}_\parallel(\mathbf{r}'_\parallel)}{|\mathbf{r}_\parallel - \mathbf{r}'_\parallel|^2} \delta\mathbf{P}_\parallel(\mathbf{r}_\parallel) = \frac{1}{2} \sum_{\mathbf{q}} \frac{1}{2\epsilon_r\epsilon_0|\mathbf{q}|} \mathbf{q} \cdot \delta\mathbf{P}_\parallel(\mathbf{q}) \mathbf{q} \cdot \delta\mathbf{P}_\parallel(-\mathbf{q}) \quad (\text{S.B6})$$

where $\delta\mathbf{P}_\parallel(\mathbf{q}) = \int d\mathbf{r}_\parallel e^{-i\mathbf{q}\cdot\mathbf{r}_\parallel} \delta\mathbf{P}_\parallel(\mathbf{r}_\parallel)$. The corresponding dispersion relation is readily identified as

$$\omega_{\mathbf{q}L} = \left(\omega_{\mathbf{q}T}^2 + \frac{|\mathbf{q}|}{2\epsilon_r\epsilon_0 m_p^\parallel} \right)^{1/2}. \quad (\text{S.B7})$$

Unlike the 3D case, the dipolar interaction lifts the longitudinal mode by a momentum-dependent term rather than a constant term.

Only the longitudinal ($\mathbf{q} \parallel \mathbf{e}_{\mathbf{q}L}$) polar phonons couple electrostatically with conduction electrons (with field operator $c_{\mathbf{k}}$ and $c_{\mathbf{k}}^\dagger$), i.e.,

$$\begin{aligned} \mathcal{H}_{\text{int}} &= -\sum_{\mathbf{q}, \sigma} \frac{ie}{2\epsilon_r\epsilon_0} \sqrt{\frac{\hbar}{2m_p^\parallel A}} \frac{\mathbf{q} \cdot \mathbf{e}_{\mathbf{q}\sigma} e^{-dq}}{q\sqrt{\omega_{\mathbf{q}\sigma}}} n(-\mathbf{q}) a_{\mathbf{q}\sigma} + h.c. \\ &= -\sum_{\mathbf{k}, \mathbf{q}} \frac{ie}{2\epsilon_r\epsilon_0} \sqrt{\frac{\hbar}{2m_p^\parallel A}} \frac{e^{-dq}}{\sqrt{\omega_{\mathbf{q}L}}} n(-\mathbf{q}) a_{\mathbf{q}L} + h.c.. \end{aligned} \quad (\text{S.B8})$$

The interaction matrix elements are similar to that of the ferrons in the main text. The drag Peltier coefficient of the polar phonons follows from Eq. (22) as

$$\begin{aligned} \pi_D &\approx \frac{e\tau_f g_\parallel \hbar^3 D_F^2}{32\delta_\nu (m_p^\parallel)^2 \epsilon_r^2 \epsilon_0^2 n_0 k_F k_B T} \int_0^{2k_F} \frac{q^2 dq}{\sqrt{1 - (q/2k_F)^2}} \frac{\cos^2(\theta/2) e^{-2dq}}{(1 + q_{TF}/q)^2} \text{csch}^2 \left(\frac{\hbar\omega_{qL}}{2k_B T} \right) \\ &\sim \text{csch}^2 \frac{\omega_{0L}}{2k_B T} \sim \frac{1}{\omega_{0L}^2}, \quad (\hbar\omega_{0L} \ll k_B T). \end{aligned} \quad (\text{S.B9})$$

Since ω_{0L} (> 10 THz) is usually much larger than the gap of the soft ferron mode (~ 2.9 THz for our studied ferroelectric at room temperature), its relative effect on the drag Peltier coefficient in ferroelectrics is small. The normal phonons also do not contribute to the critical enhancement of the transport coefficients at the phase transition. Moreover, the harmonic polar phonons do not carry electric dipoles, so ω_{0L} does not experience a Stark shift by an external electric field.

Eq. (20) in the main text remains valid for a polar dielectric/graphene bilayer without ferrons, but ω_q is then the frequency dispersion of the out-of-plane optical phonons, and should be added to Eq. (S.B9) for the total effect.

[1] E. H. Hwang and S. D. Sarma, Acoustic phonon scattering limited carrier mobility in two-dimensional extrinsic graphene, Phys. Rev. B **77**, 115449 (2008).